Journal of Southeast University (English Edition) Vol. 31, No. 4, pp. 522 - 528 Dec. 2015 ISSN 1003—7985

Ultimate load bearing capacity evaluation of concrete beams subjected to freeze-thaw cycles

Qin Xiaochuan[1] Meng Shaoping[1] Tu Yongming[1] Cao Dafu[2]

([1]School of Civil Engineering, Southeast University, Nanjing 210096, China)

([2]College of Civil Science and Engineering, Yangzhou University, Yangzhou 225127, China)

Abstract: A theoretical prediction method based on the change of concrete material is proposed to evaluate the ultimate bending moment of concrete beams which have undergone freeze-thaw cycles (FTCs). First, the freeze-thaw damage on concrete material is analyzed and the residual compressive strength is chosen to indicate the freeze-thaw damage. Then, the equivalent block method is employed to simplify the compressive stress-strain curve of the freeze-thaw damaged concrete and the mathematical expression for the ultimate bending moment is obtained. Comparisons of the predicted results with the test data indicate that the ultimate bending moment of concrete beams affected by FTC attack can be predicted by this proposed method. However, the bond-slip behavior and the randomness of freeze-thaw damage will affect the accuracy of the predicted results, especially when the residual compressive strength is less than 50%.

Key words: concrete beam; freeze-thaw cycles; ultimate bending moment; structural analysis

doi: 10.3969/j.issn.1003-7985.2015.04.016

The freeze-thaw cycle (FTC) attack is one of the most severe factors that lead to the durability deterioration of existing reinforced concrete structures in cold regions[1-2]. As FTCs are repeated, the concrete material gradually loses its strength and stiffness with the growth of the internal cracks caused by the volume expansion of freezing water stored in the pore system of concrete[3-4]. Several reports have been focused on the performance of concrete material under FTCs[5-12]. However, little attention was paid to reinforced concrete members and prestressed concrete members[13-15]. For concrete structures, concrete material deterioration will cause load-bearing capacity degradation, which eventually makes the whole structure incapable of service. Thus, there is a growing need for methods to evaluate the freeze-thaw damaged concrete structures. A method for predicting the ultimate load bearing capacity of freeze-thaw damaged concrete structures is proposed, testified and discussed in this paper.

Received 2015-02-09.

Biographies: Qin Xiaochuan (1985—), male, graduate; Tu Yongming (corresponding author), male, doctor, associate professor, tuyongming@seu.edu.cn.

Foundation items: The National Natural Science Foundation of China (No. 50978224, 51378104), the Priority Academic Program Development of Jiangsu Higher Education Institutions.

Citation: Qin Xiaochuan, Meng Shaoping, Tu Yongming, et al. Ultimate load bearing capacity evaluation of concrete beams subjected to freeze-thaw cycles[J]. Journal of Southeast University (English Edition), 2015, 31(4): 522 - 528. [doi: 10.3969/j.issn.1003-7985.2015.04.016]

1 Foundations of the Prediction Method

1.1 Indicators of freeze-thaw damage

In the assessment of the freeze-thaw damage on concrete, various indicators, such as the relative dynamic modulus of elasticity (RDME), compressive strength and etc., must be measured after a specified number of FTCs.

The RDME is the most popular indicator of freeze-thaw damage in many test standards, such as ASTM C666/C666M-03[16], GB/T 50082—2009[17], etc. The test of RDME is developed from the analysis of a homogeneous rod under free flexural vibration. Thus, it is assumed that the specimen is homogeneous and elastic. However, this assumption is not quite true for concrete material, especially for freeze-thaw damaged concrete material. For undamaged concrete material, as shown in Fig. 1(a), the assumption is reasonable because the whole specimen is tightly bound by cementitious materials and the volume ratio of the micro-cracks to the specimen is very low, which means that vibration can be transmitted through the specimen easily. For freeze-thaw damaged concrete material, as shown in Fig. 1(b), the situation is different. As FTCs go on, the original micro-cracks will grow larger and new cracks will form. Hence, the specimen will be separated into a few micro-units and cannot be treated as a homogeneous material any more.

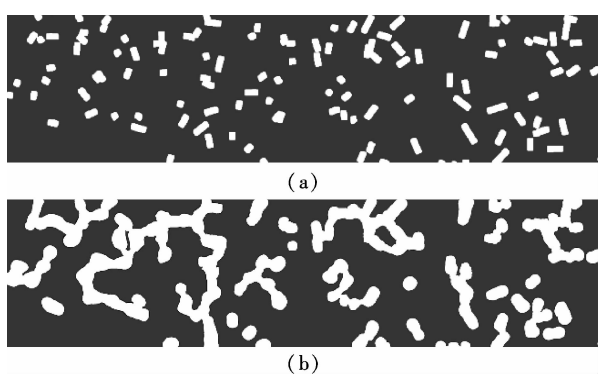

Fig. 1 Development of micro-cracks inside the specimen under FTCs. (a) Undamaged status; (b) Damaged status

Another feasible indicator of freeze-thaw damage is the compressive strength of the freeze-thaw damaged concrete cube. In the compression test, it is appropriate to assume that the undamaged concrete material is homogeneous because the micro-cracks tend to close under compression. When performing the compression test on the freeze-thaw damaged concrete cube, it is still reasonable to believe that the specimen is homogeneous, because some of the cracks induced by FTCs (i. e. horizontal cracks) will first be compacted by the compressive force from the test machine before the concrete cubic is ruptured, which can be regarded as a process of "crack closure" (see Fig. 2)[18]. In the compressive stress-strain curves of the freeze-thaw damaged concrete, the initial parts of the ascending branches are not so steep as the following parts of these ascending branches, revealing a "crack closure".

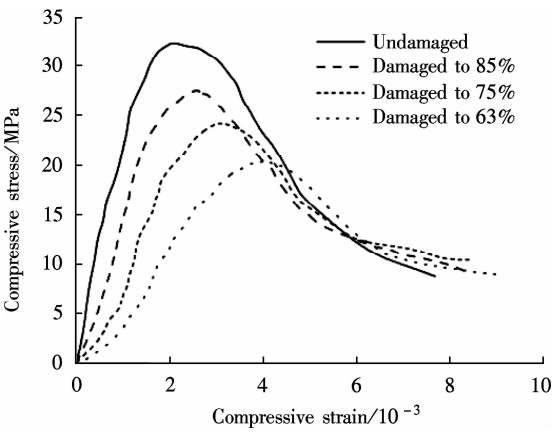

Fig. 2 Stress-strain relationship under compression

Comparing the two indicators mentioned above, the compressive strength is better than the RDME theoretically. In addition, the RDME tends to recover itself if it is not measured timely, especially in high-strength concrete. However, the compressive strength varies relatively little as time goes on[19]. Last but not least, the compressive strength is a more effective indicator, which directly affects the behaviors of the freeze-thaw damaged concrete structures.

1.2 Uniaxial compression behavior after FTCs

There are lots of internal micro-cracks, mainly existing in the paste and paste-aggregate interfaces when concrete hardens even if there is not any load or environmental effect. When submerged into water, these cracks will suck water into the concrete pore system. As the temperature drops below the freezing point, water will turn into ice accompanied by a 9% volume increase, which causes tensile stress inside the concrete. If the tensile stress exceeds the tensile strength of concrete material, new internal cracks will initiate and the old ones will open wider. As FTCs are repeated, more and more water will be absorbed into the concrete during thawing, causing larger expansion and more internal cracks during the next freezing process. The load carrying area will decrease with the formation and growth of internal cracks, which leads to a decrease in the compressive strength. Since there are less micro-units to carry the load, each unit will reach its elastic limit more quickly. Hence, the compressive behavior of concrete becomes softer. The peak compressive strength and the Young's modulus decrease, while the peak compressive strain and the ultimate compressive strain increase (see Fig. 2)[18]. The damage level in Fig. 2[18] is re-rated in terms of residual compressive strength.

2 Theoretical Prediction Method

2.1 General considerations

Based on Refs. [15, 19], the theoretical prediction is carried out by the following assumptions:

1) Plane sections before bending remain plane after bending. This assumption is proved to be true in Ref. [15].

2) The tensile strength of the concrete may be neglected. Due to freeze-thaw damage and the low tensile strength of the undamaged concrete, the freeze-thaw damaged concrete can barely carry tension.

3) The simplified stress-strain curve of the freeze-thaw damaged concrete is shown in Fig. 3 and the curve is determined by

$$\sigma_c = f_c^{FT}\left[1-\left(1-\frac{\varepsilon_c}{\varepsilon_0^{FT}}\right)^{n^{FT}}\right] \qquad 0 \leqslant \varepsilon_c \leqslant \varepsilon_0^{FT} \tag{1}$$

$$\sigma_c = f_c^{FT} \qquad \varepsilon_0^{FT} < \varepsilon_c \leqslant \varepsilon_{cu}^{FT} \tag{2}$$

$$\varepsilon_0^{FT} = [0.002 + 0.5(f_{cu,k} - 50) \times 10^{-5}] \cdot \left(\frac{f_c^{FT}}{f_c}\right)^{-(17.208\,5\exp(-(f_{cu,k}/7.139\,24))+1.303\,96)} \tag{3}$$

$$\varepsilon_{cu}^{FT} = 0.003\,3 - (f_{cu,k}^{FT} - 50) \times 10^{-5} \qquad \varepsilon_{cu}^{FT} \geqslant \varepsilon_0^{FT} \tag{4}$$

$$n^{FT} = 2 - \frac{1}{60}(f_{cu,k}^{FT} - 50) \tag{5}$$

where ε_c is the compressive strain in the concrete; σ_c is the compressive stress corresponding to ε_c; f_c is the

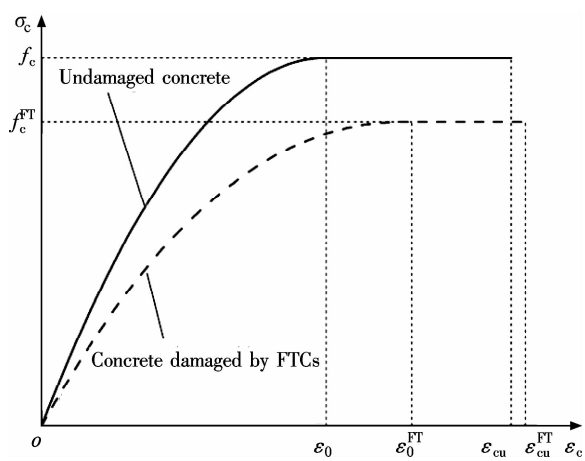

Fig. 3 Compressive stress-strain curve of concrete

compressive strength of the undamaged concrete; f_c^{FT} is the compressive strength of concrete after FTCs; ε_0^{FT} is the peak strain when the stress is equal to f_c^{FT}; ε_{cu}^{FT} is the ultimate strain of the freeze-thaw damaged concrete; $f_{cu,k}$ is the characteristic compressive strength of the undamaged concrete cube; $f_{cu,k}^{FT}$ is the characteristic compressive strength of the concrete cube after FTCs; n^{FT} is a coefficient.

The former tests performed by our team show that the peak compressive strength and the Young's modulus decrease, while the peak compressive strain and the ultimate compressive strain increase[18]. Therefore, the stress-strain curve, especially the peak strain ε_0^{FT} and the ultimate strain ε_{cu}^{FT} of the freeze-thaw damaged concrete, need improvements. The modified ε_0^{FT} consists of two parts, i.e. the peak strain of the undamaged concrete $\varepsilon_0 = 0.002 + 0.5(f_{cu,k} - 50) \times 10^{-5}$ and the correction factor $k = (f_c^{FT}/f_c)^{-(17.208\,5\exp(-(f_{cu,k}/7.139\,24))+1.303\,96)}$. This correction factor is derived from the nonlinear fitting of the test results in Ref. [18]. With freeze-thaw deterioration, ε_{cu}^{FT} will also increase with the decrease of $f_{cu,k}^{FT}$. However, the increasing rate of ε_{cu}^{FT} is slower than that of ε_0^{FT}. In the extreme case, ε_0^{FT} is equal to ε_{cu}^{FT}. Hence, it is necessary to limit $\varepsilon_{cu}^{FT} \geqslant \varepsilon_0^{FT}$.

4) The stress-strain curve for steel is perfect elasto-plastic, and the ultimate strain is 0.01. Commonly, FTCs have little effect on steel, which substantiates this assumption.

2.2 Ultimate load bearing capacity

In order to simplify the mathematical expression, the actual shape of concrete compressive stress block is replaced by an equivalent rectangle. The equivalent rectangle has the same area and point of action as the actual concrete compressive stress block[20]. Therefore, the freeze-thaw damaged equivalent parameter α_1^{FT} is calculated as

$$\alpha_1^{FT} = \frac{\left(1 - \frac{1}{n^{FT}+1}\frac{\varepsilon_0^{FT}}{\varepsilon_{cu}^{FT}}\right)^2}{\frac{2}{(n^{FT}+1)(n^{FT}+2)}\left(\frac{\varepsilon_0^{FT}}{\varepsilon_{cu}^{FT}}\right)^2 - \frac{2}{n^{FT}+1}\frac{\varepsilon_0^{FT}}{\varepsilon_{cu}^{FT}} + 1} \quad (6)$$

Then, based on the classic formulae of material mechanics with minor adjustments, the ultimate load bearing capacity of the freeze-thaw damaged beam can be calculated as

$$\alpha_1^{FT} f_c^{FT} bx = f_y A_s - f'_y A'_s + f_{py} A_p + (\sigma'_{p0} - f'_{py}) A'_p \quad (7)$$

$$M_u^{FT} = \alpha_1^{FT} f_c^{FT} bx\left(h_0 - \frac{x}{2}\right) + f'_y A'_s (h_0 - a'_s) - (\sigma'_{p0} - f'_{py}) A'_p (h_0 - a'_p) \quad (8)$$

where b is the beam width; x is the height of equivalent rectangular stress block; f_y is the tensile strength of the steel bar; f'_y is the compressive strength of the steel bar; f_{py} is the tensile strength of the prestressed tendon; f'_{py} is the compressive strength of the prestressed tendon; σ'_{p0} is the stress of the prestressed tendon when the stress of concrete at this layer is equal to zero; A_s is the cross-section area of the tensile steel bar; A'_s is the cross-section area of the compressive steel bar; A_p is the cross-section area of the tensile prestressed tendon; A'_p is the cross-section area of the tensile prestressed tendon; M_u^{FT} is the ultimate bending moment of the freeze-thaw damaged beam; h_0 is the effective height; a'_s is the distance from the action point of the compressive steel bar to the edge of the compressive stress block; a'_p is the distance from the action point of the compressive prestressed tendon to the edge of the compressive stress block.

3 Verification Tests

3.1 Materials

Two concrete mix designs (named type A and type B) are used. The components and mix designs for the concrete materials are described in Tab. 1 and Tab. 2.

Tab. 1 Materials used for the concrete mix

Components	Materials
Cement	P · O, 42.5R cement
Water	Tap water
Fine aggregates	River sand, fineness module 2.6
Coarse aggregates	Crushed stone, 5 to 31.5 mm
Fly ash	Class Ⅱ fly ash
Additives	JM-9 composite water reducing agent

Tab. 2 Concrete mix designs and basic properties

Ingredients and basic properties	Type A	Type B
C/(kg · m^{-3})	463	380
Water-cement ratio	0.38	0.46
S/(kg · m^{-3})	599	712
G/(kg · m^{-3})	1 139	1 103
F/(kg · m^{-3})	62	50
A/(kg · m^{-3})	8.93	6.02
Air content of fresh concrete/%	2.8	3.0
Compressive strength/MPa	80.3	69.0

Hot-rolled ribbed steel bars (HRB335) of either 10 or 8 mm diameter were used as the longitudinal reinforcement. The stirrup was a cold-drawn wire with a diameter of 4 mm. The prestressed reinforcement was a 5 mm low-relaxation steel wire with a nominal ultimate strength of 1 570 MPa. The physical and mechanical properties of these reinforcements are shown in Tab. 3.

3.2 Specimens

For each type of concrete, four kinds of specimens were prepared:

1) Twelve cubic specimens (100 mm × 100 mm × 100 mm), three as a group, were used to test the residual compressive strength after a specified number of FTCs.

Tab. 3 Physical and mechanical properties of the reinforcements

Reinforcements	Diameter/mm	Yield strength/MPa	Ultimate strength/MPa	Young's modulus/GPa
Steel bar	10	373	526	186
	8	360	517	176
Stirrup	4	462	569	187
Prestressed wire	5	1 550	1 624	198

2) Three prismatic specimens (400 mm × 100 mm × 100 mm) were used to test RDME during FTCs.

3) Twelve prestressed concrete beams with straight prestressed wires, three as a group, were used to test the bending response after specified number of FTCs (see Fig. 4(a)).

4) Twelve prestressed concrete beams with curved prestressed wires, three as a group, were also used to test the bending response after specified number of FTCs (see Fig. 4(b)).

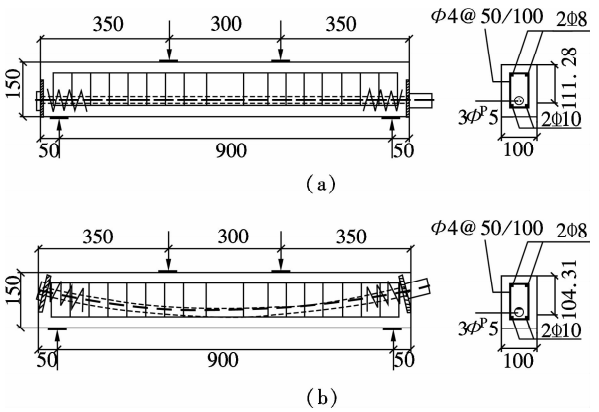

Fig. 4 Prestressed concrete beam (unit: mm). (a) With straight prestressed wires; (b) With curved prestressed wires

3.3 Program

The freeze-thaw test followed the Procedure A in ASTM C666/C666M-03[16]. In this procedure of rapid freeze-thaw in water, the temperature of the specimen was decreased from 5 to −16 ℃ and then increased from −16 to 5 ℃ over a period of 2.8 h, during which the cooling time took 2.0 h and heating took 0.8 h; i.e. 28.6 % of the time was used for thawing. Moreover, the time taken to decrease the core temperature of the specimen from 3 to −16 ℃ was about 1.7 h, and to increase it from −16 to 3 ℃ was 0.75 h. The period of transition between the freezing and thawing phases of the cycle was 5 min. All specimens were tested after 0, 75, 100, 125 FTCs, respectively.

4 Results and Discussion

4.1 Compressive strength and RDME

The test results of the RDME and the residual compressive strength are shown in Fig. 5. The compressive strength of type A and type B concrete decrease in a similar way. However, the RDME of type A does not decrease obviously before 100 FTCs, while the RDME of type B remains only 3% after 125 FTCs. For type A concrete, the compressive strength drops faster than the RDME. On the contrary, for type B concrete, the RDME drops faster than the compressive strength. This reinforces that the compressive strength may be a better indicator of freeze-thaw damage.

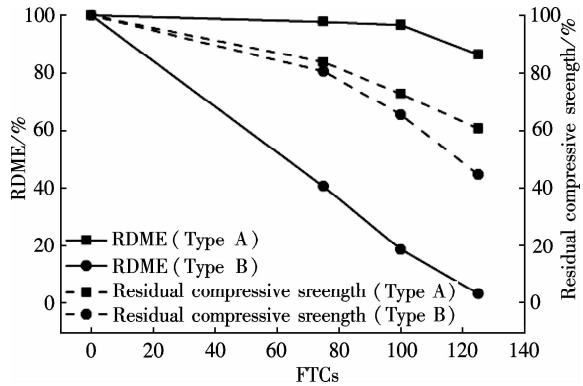

Fig. 5 Test results of concrete material damaged by FTCs

4.2 Ultimate bending moment

The test results of this experiment as well as those of the experiments performed by others [21-22] are listed in Tab. 4. The predicted results calculated from Eqs. (3) to (8) are shown in Tab. 4.

From Tab. 4, it is clear that FTCs reduce the compressive strength of concrete material, which lead to a reduction in the load bearing capacity, and this trend is sharper when the concrete damage aggravates. The layout of prestressed wire affects the load bearing capacity most when the concrete is slightly damaged; however, as damage goes on, the effect of concrete type becomes more and more dominant. Moreover, the experimental results suggest that the prestressed concrete beam with higher strength concrete and curved prestressed wire performs better under FTCs.

4.3 Comparison and discussion

The reliability of the proposed method for predicting the load bearing capacity of freeze-thaw damaged beams is shown in Fig. 6. Results show that the failure load is better estimated while the concrete strength remains more than 50%. More than half of the predicted results are on the safe side ($M_{u,num}/M_{u,exp} \leqslant 1$), and most of the prediction errors remain less than 10%. In other words, if the margin of error is ± 10%, the predicted results are reliable except for damaged beam HD2.

The overestimation of HD2 is 46%, which is larger than the FEM result in Ref. [14]. This is partly because of the bond-slip behavior which might exist in concrete

Tab. 4 Summary of beam test results

Reference	Name	Length/ m	$h \times b$/ (mm × mm)	h_0/ mm	$f_{cu,m}^{FT}$/ MPa	$f_{cu,k}^{FT}$/ MPa	$f_{c,m}^{FT}$/ MPa	Steel bar/ mm	Stirrup/ mm	$M_{u,exp}$/ (kN · m)	$M_{u,num}$/ (kN · m)
This paper	QR1	1.0	150 × 100	111.28	80.3	61.9	51.5	2ϕ10 + 3ϕ5	18ϕ4	14.55	14.28
	QD1-1	1.0	150 × 100	111.28	67.3	50.7	43.5	2ϕ10 + 3ϕ5	18ϕ4	14.28	14.01
	QD1-2	1.0	150 × 100	111.28	58.4	43.5	38.6	2ϕ10 + 3ϕ5	18ϕ4	14.20	13.78
	QD1-3	1.0	150 × 100	111.28	48.7	35.7	32.6	2ϕ10 + 3ϕ5	18ϕ4	14.02	13.40
	QR2	1.0	150 × 100	104.31	80.3	61.9	51.5	2ϕ10 + 3ϕ5	18ϕ4	11.92	13.23
	QD2-1	1.0	150 × 100	104.31	67.3	50.7	43.5	2ϕ10 + 3ϕ5	18ϕ4	11.87	12.97
	QD2-2	1.0	150 × 100	104.31	58.4	43.5	38.6	2ϕ10 + 3ϕ5	18ϕ4	11.85	12.73
	QD2-3	1.0	150 × 100	104.31	48.7	35.7	32.6	2ϕ10 + 3ϕ5	18ϕ4	11.74	12.36
	QR3	1.0	150 × 100	111.28	69.0	52.1	44.6	2ϕ10 + 3ϕ5	18ϕ4	12.99	14.09
	QD3-1	1.0	150 × 100	111.28	55.6	41.3	37.1	2ϕ10 + 3ϕ5	18ϕ4	12.75	13.49
	QD3-2	1.0	150 × 100	111.28	45.2	32.8	30.2	2ϕ10 + 3ϕ5	18ϕ4	12.58	13.25
	QD3-3	1.0	150 × 100	111.28	30.8	20.4	20.6	2ϕ10 + 3ϕ5	18ϕ4	12.19	12.18
	QR4	1.0	150 × 100	104.31	69.0	52.1	44.6	2ϕ10 + 3ϕ5	18ϕ4	11.87	13.05
	QD4-1	1.0	150 × 100	104.31	55.6	41.3	37.1	2ϕ10 + 3ϕ5	18ϕ4	11.81	12.71
	QD4-2	1.0	150 × 100	104.31	45.2	32.8	30.2	2ϕ10 + 3ϕ5	18ϕ4	11.70	12.21
	QD4-3	1.0	150 × 100	104.31	30.8	20.4	20.6	2ϕ10 + 3ϕ5	18ϕ4	11.46	11.13
Ref. [21]	HR1	4.4	500 × 200	430	56.2	41.8	37.6	4ϕ20	28ϕ8	317.1	313.52
	HD1	4.4	500 × 200	430	26.2	16.5	17.5	4ϕ20	28ϕ8	259.3	252.0
	HR2	3.0	300 × 200	260	56.2	41.8	37.6	3ϕ20	18ϕ8	135.5	136.91
	HD2	3.0	300 × 200	260	26.2	16.5	17.5	3ϕ20	18ϕ8	70.0	102.3
	HR3	4.4	500 × 200	430	56.2	41.8	37.6	6ϕ20	32ϕ8	411.4	434.03
	HD3	4.4	500 × 200	430	26.2	16.5	17.5	6ϕ20	32ϕ8	276.3	295.6
	HR4	3.0	300 × 200	260	56.2	41.8	37.6	5ϕ20	22ϕ8	162.5	166.42
	HD4	3.0	300 × 200	260	26.2	16.5	17.5	5ϕ20	22ϕ8	66.0	70.3
Ref. [22]	GR1	1.0	150 × 100	120	45.8	33.3	30.6	2ϕ10	16ϕ4	7.15	6.45
	GD1-1	1.0	150 × 100	120	39.4	27.8	26.4	2ϕ10	16ϕ4	6.90	6.36
	GD1-2	1.0	150 × 100	120	32.1	21.5	21.5	2ϕ10	16ϕ4	6.64	6.18
	GD1-3	1.0	150 × 100	120	25.2	15.7	16.9	2ϕ10	16ϕ4	6.26	5.93
	GR2	1.0	150 × 100	120	45.8	33.3	30.6	2ϕ12	16ϕ4	11.35	11.22
	GD2-1	1.0	150 × 100	120	39.4	27.8	26.4	2ϕ12	16ϕ4	11.08	10.87
	GD2-2	1.0	150 × 100	120	32.1	21.5	21.5	2ϕ12	16ϕ4	10.68	10.23
	GD2-3	1.0	150 × 100	120	25.2	15.7	16.9	2ϕ12	16ϕ4	10.01	9.34
	GR3	1.0	150 × 100	120	51.5	38.0	34.4	2ϕ12	16ϕ4	11.52	11.44
	GD3-1	1.0	150 × 100	120	44.8	32.4	30.0	2ϕ12	16ϕ4	11.25	11.15
	GD3-2	1.0	150 × 100	120	37.1	25.8	24.8	2ϕ12	16ϕ4	10.89	10.64
	GD3-3	1.0	150 × 100	120	29.9	19.6	20.0	2ϕ12	16ϕ4	10.41	9.94
	GR4	1.0	150 × 100	120	51.5	38.0	34.4	2ϕ14	16ϕ4	12.57	12.58
	GD4-1	1.0	150 × 100	120	44.8	32.4	30.0	2ϕ14	16ϕ4	12.26	12.21
	GD4-2	1.0	150 × 100	120	37.1	25.8	24.8	2ϕ14	16ϕ4	11.70	11.57
	GD4-3	1.0	150 × 100	120	29.9	19.6	20.0	2ϕ14	16ϕ4	10.90	10.69

Notes: 1) The letter "R" in names represents the undamaged beam. 2) h and b are the height and width of the cross-section; h_0 is the effective height; $f_{cu,m}^{FT}$ is the mean compressive strength of the concrete cube after FTCs; $f_{cu,k}^{FT}$ is the characteristic compressive strength of the concrete cube after FTCs; $f_{c,m}^{FT}$ is the mean compressive strength of concrete after FTCs; $M_{u,exp}$ is the ultimate bending moment of the tested specimens; $M_{u,num}$ is the ultimate bending moment predicted by Eqs. (3) to (8). 3) The yield stresses of the steel bars are 670 MPa for ϕ 20 mm in Ref. [21], 373 MPa for ϕ10 mm, 489 MPa for ϕ12 mm and 402 MPa for ϕ14 mm in Ref. [22].

beams with damage of more than 50% by FTCs. Moreover, it is reported that the freeze-thaw induced cracks of HD2 were mostly parallel to the longitudinal axis of beams, which have a decisive influence on the fracture of concrete in compression[21]. These may account for the disagreement between the theoretical and experimental results of HD2.

The load bearing capacity of freeze-thaw damaged beams can be evaluated following the method presented in this paper. The compressive stress-strain behavior of concrete blocks is the key to the load bearing capacity prediction. For most reinforced and prestressed concrete beams, the compressive behavior of concrete can be easily obtained through drilled concrete cores from the main structure or pre-casted blocks which experienced the same environmental condition as the main structure. Thereafter,

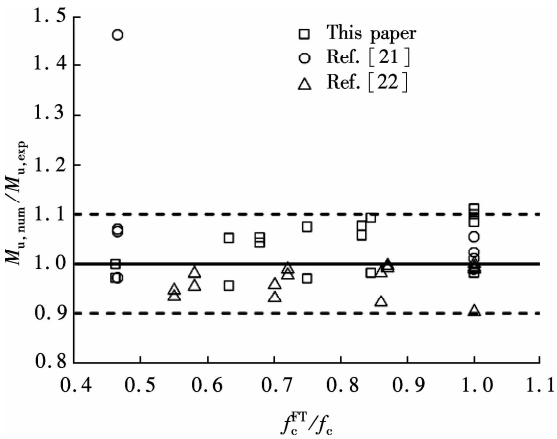

Fig. 6 Comparison of results from experiments and theoretical predictions

the ultimate load bearing capacity can be calculated by Eqs. (7) and (8), which is familiar to most civil engineers. Though the prediction method is reliable for most of the concrete beams when the concrete strength loss due to FTCs is less than 50%, it is significant that bond-slip behavior will influence the accuracy of the prediction when the compressive strength loss is more than 50%. The size-effect of freeze-thaw damage was not researched thoroughly, but Ref. [23] showed that the frost-damage might significantly differ at various distances from the exposed surface. Thus, when evaluating concrete structures with larger sections, frost-damage distribution is an important factor.

5 Conclusions

1) The compressive strength of concrete is proved to be a better indicator of freeze-thaw damage on concrete material than RDME.

2) Based on the characteristics of the compressive stress-strain curve of freeze-thaw damaged concrete, a theoretical method to predict the ultimate bending moment is proposed.

3) Comparisons of the predicted results with the experimental data show that the load bearing capacity of freeze-thaw damaged beams can be predicted by the proposed method.

4) Two factors, the bond-slip behavior and the frost-damage distribution, affect the prediction of the failure load, especially when the residual compressive strength is less than 50%.

References

[1] Pigeon M, Pleau R. *Durability of concrete in cold climates*[M]. Taylor & Francis, 1995.

[2] Fagerlund G. Modeling the service life of concrete exposed to frost[C]//*International Conference on Ion and Mass Transport in Cement-Based Materials*. Toronto, Canada, 1999: 195 - 204.

[3] Cho T. Prediction of cyclic freeze-thaw damage in concrete structures based on response surface method[J]. *Construction & Building Materials*, 2007, **21**(12): 2031 - 2040.

[4] Ueda T, Wang L, Hasan M, et al. Mesoscale simulation of influence of frost damage on mechanical properties of concrete[J]. *Journal of Materials in Civil Engineering*, 2009, **21**(6): 244 - 252.

[5] Duan A, Jin W L, Qian J R. Effect of freeze-thaw cycles on the stress-strain curves of unconfined and confined concrete[J]. *Materials and Structures*, 2011, **44**(7): 1309 - 1324.

[6] Hasan M, Ueda T, Sato Y. Stress-strain relationship of frost-damaged concrete subjected to fatigue loading[J]. *Journal of Materials in Civil Engineering*, 2008, **20**(1): 37 - 45.

[7] Li W T, Sun W, Jiang J Y. Damage of concrete experiencing flexural fatigue load and closed freeze/thaw cycles simultaneously[J]. *Construction & Building Materials*, 2011, **25**(5): 2604 - 2610.

[8] Shang H S, Song Y P. Experimental study of strength and deformation of plain concrete under biaxial compression after freezing and thawing cycles[J]. *Cement & Concrete Research*, 2006, **36**(10): 1857 - 1864.

[9] Shang H S, Song Y P, Qin L K. Experimental study on the property of concrete after freeze-thaw cycles[J]. *China Concrete and Cement Products*, 2005, **32**(2): 9 - 11. (in Chinese)

[10] Shang H S, Song Y P, Qin L K. Experimental study on strength and deformation of plain concrete under triaxial compression after freeze-thaw cycles[J]. *Building & Environment*, 2008, **43**(7): 1197 - 1204.

[11] Shang H S, Yin Q X, Song Y P, et al. Experimental study on the influence of freezing and thawing cycles on deformation features of common concrete[J]. *Yangtze River*, 2006, **39**(4): 60 - 63. (in Chinese)

[12] Sun W, Zhang Y M, Yan H D, et al. Damage and damage resistance of high strength concrete under the action of load and freeze-thaw cycles[J]. *Cement & Concrete Research*, 1999, **29**(9): 1519 - 1523.

[13] Diao B, Sun Y, Cheng S H, et al. Effects of mixed corrosion, freeze-thaw cycles, and persistent loads on behavior of reinforced concrete beams[J]. *Journal of Cold Regions Engineering*, 2011, **25**(1): 37 - 52.

[14] Hanjari K Z, Kettil P, Lundgren K. Modelling the structural behaviour of frost-damaged reinforced concrete structures[J]. *Structure and Infrastructure Engineering*, 2013, **9**(5): 416 - 431.

[15] Cao D F, Qin X C, Yuan S F. Experimental study on mechanical behaviors of prestressed concrete beams subjected to freeze-thaw cycles[J]. *China Civil Engineering Journal*, 2013, **46**(8): 38 - 44. (in Chinese)

[16] ASTM. ASTM C666/C666M-03 Standard test method for resistance of concrete to rapid freezing and thawing [S]. ASTM, 2008.

[17] Ministry of Housing and Urban-Rural Development of the People's Republic of China. GB/T 50082—2009 Standard for test methods of long-term performance and durability of ordinary concrete[S]. Beijing: China Architecture & Building Press, 2009. (in Chinese)

[18] Cao D F, Fu L Z, Yang Z W, et al. Study on constitu-

tive relations of compressed concrete subjected to action of freezing-thawing cycles[J]. *Journal of Building Materials*, 2013, **16**(1): 17-23, 32. (in Chinese)
[19] Jacobsen S, Sellevold J. Self healing of high strength concrete after deterioration by freeze/thaw[J]. *Cement & Concrete Research*, 1996, **26**(1): 55-62.
[20] Guo Z H. *The strength and the constitutive relation of concrete: theory and application*[M]. Beijing: China Architecture & Building Press, 2004. (in Chinese)
[21] Hassanzadeh M, Fagerlund G. Residual strength of the frost-damaged reinforced concrete beams[C]//*European Conference on Computational Mechanics*. Lisbon, Portugal, 2006: 366-366.
[22] Guo R Y. Experimental research on reinforced concrete bending members under freeze-thaw cycles[D]. Yangzhou: School of Civil Engineering, Yangzhou University, 2011. (in Chinese)
[23] Petersen L, Lohaus L, Polak M A. Influence of freezing-and-thawing damage on behavior of reinforced concrete elements[J]. *ACI Materials Journal*, 2007, **104**(4): 369-378.

冻融循环损伤后混凝土梁的极限承载力分析

秦晓川[1] 孟少平[1] 涂永明[1] 曹大富[2]

([1] 东南大学土木工程学院, 南京 210096)
([2] 扬州大学建筑科学与工程学院, 扬州 225127)

摘要:为了预测冻融循环损伤后混凝土梁的受弯极限承载能力,提出一种基于混凝土材性变化的预测方法. 该方法首先分析混凝土材料受冻融循环损伤的特点,并提出将冻融循环损伤后混凝土的抗压强度作为损伤指标,然后通过图形等效的方法来简化冻融损伤后混凝土的受压应力-应变曲线,推导出受弯极限承载力计算公式. 理论预测结果和试验实测数据表明,该预测方法能够有效地预测冻融循环损伤后混凝土梁的极限荷载. 但是当混凝土残余抗压强度小于50%时,由于黏结滑移现象以及冻融循环损伤的随机性,预测结果的精确性将下降.

关键词:混凝土梁;冻融循环;极限弯矩;结构分析
中图分类号:TU378.2